

Study of the neutron-rich nucleus ^{36}Si

X. Liang,^{1,*} F. Azaiez,³ R. Chapman,¹ F. Haas,² D. Bazzacco,⁸ S. Beghini,⁸ B. R. Behera,⁶ L. Berti,⁶ M. Burns,¹ E. Caurier,² L. Corradi,⁶ D. Curien,² A. Deacon,⁷ G. de Angelis,⁶ Zs. Dombradi,⁹ E. Farnea,⁸ E. Fioretto,⁶ A. Hodsdon,¹ A. Gadea,⁶ F. Ibrahim,³ A. Jungclaus,⁴ K. Keyes,¹ A. Latina,⁶ S. Lunardi,⁸ N. Marginean,⁶ R. Menegazzo,⁸ G. Montagnoli,⁸ D. R. Napoli,⁶ F. Nowacki,² J. Ollier,¹ A. Papenberg,¹ G. Pollarolo,¹⁰ V. F. E. Pucknell,¹² M.-D. Salsac,² F. Scarlassara,⁸ J. F. Smith,⁷ K. Spohr,¹ M. Stanoiu,³ A. M. Stefanini,⁶ S. Szilner,^{6,11} N. Toniolo,⁶ M. Trotta,⁶ D. Verney,⁵ Z. Wang,⁶ and J. Wrzesinski¹³

¹*School of Engineering and Science, University of Paisley, Paisley, PA1 2BE, United Kingdom*

²*IPHC, UMR 7500, CNRS-IN2P3 and Université Louis Pasteur, F-67037 Strasbourg Cedex 2, France*

³*IPN, IN2P3-CNRS and Université Paris-Sud, F-91406 Orsay Cedex, France*

⁴*Dep. de Física Teórica, Universidad Autónoma de Madrid, E-28049 Madrid, Spain*

⁵*Ganil, BP 5027, F-14021 Caen Cedex, France*

⁶*INFN, Laboratori Nazionali di Legnaro, I-35020 Legnaro, Padova, Italy*

⁷*Schuster Laboratory, University of Manchester, Manchester, M13 9PL, United Kingdom*

⁸*Dipartimento di Fisica and INFN-Sezione di Padova, Università di Padova, I-35131 Padova, Italy*

⁹*ATOMKI, P.O. Box 51, H-4001 Debrecen, Hungary*

¹⁰*Dipartimento di Fisica Teorica, Università di Torino and INFN Sez di Torino, Via P. Giuria 1, I-10125 Torino, Italy*

¹¹*Ruder Bosković Institute, Zagreb, Croatia*

¹²*CCLRC Daresbury Laboratory, Warrington, WA4 4AD, United Kingdom*

¹³*Henryk Niewodniczanski Institute of Nuclear Physics, ul. Radzikowskiego 152, PL-31342 Krakow, Poland*

(Received 21 April 2006; published 17 July 2006)

Excited states of $N = 22$ ^{36}Si , populated in deep-inelastic processes produced by the interaction of a 215 MeV beam of ^{36}S ions with a ^{208}Pb target, were studied in the present work. γ rays from the binary fragments detected using CLARA, an array of 25 Ge Clover detectors, were measured in coincidence with projectile-like fragments detected by PRISMA, a large solid angle magnetic spectrometer. Two new γ -ray photopeaks at energies of 1442 and 842 keV were observed and tentatively assigned to the $4^+ \rightarrow 2^+$ and $6^+ \rightarrow 4^+$ transitions, respectively. The systematics of the level structures of $N = 22$ isotones are presented, and a comparison is made of the behavior of Si, Mg, and S isotopes. The level structure of ^{36}Si is also compared with the results of *sdpf* shell model calculations.

DOI: [10.1103/PhysRevC.74.014311](https://doi.org/10.1103/PhysRevC.74.014311)

PACS number(s): 23.20.Lv, 25.70.Lm, 27.30.+t

I. INTRODUCTION

The region of neutron-rich nuclei around $N = 20$ is the subject of active research, both experimental and theoretical, since this is the region in which the breaking of a semimagic shell closure far from stability was first detected. A large quadrupole deformation in $N = 20$ ^{32}Mg has been inferred from measurements of $B(E2; 0^+ \rightarrow 2^+)$ [1–3]. The well-known “island of inversion” [4] around ^{31}Na and ^{32}Mg has been interpreted within a shell model context as arising from a 2p-2h intruder configuration, intrinsically deformed [5].

Experimental measurement of excitation energies and $B(E2; 0^+ \rightarrow 2^+)$ values for the first 2^+ states of neutron-rich S isotopes populated using relativistic Coulomb excitation [6, 7] indicate that $^{40,42,44}\text{S}$ are deformed ($\beta_2 \sim 0.3$) in agreement with theoretical calculations by Werner *et al.* [8]. In relation to these observations, our previous deep-inelastic work [9, 10] has shown that the $3/2^+$ and $1/2^+$ levels of the odd- A neutron-rich Cl isotopes come closer in energy and eventually cross at ^{41}Cl ($N = 24$) as the occupation of the $1f_{7/2}$ neutron shell

increases. Indeed, the near-degeneracy of the $1d_{3/2}$ and $2s_{1/2}$ proton orbitals is the determining factor for the onset of deformation in neutron-rich sulfur isotopes with $N = 24$ and 26 [11].

Between Mg and S, the neutron-rich Si isotopes have also attracted intense interest. Measurements of $B(E2; 0^+ \rightarrow 2^+)$ values and the energies of first 2^+ states for $^{32,34,36,38}\text{Si}$ have been reported in Ref. [12]. The systematic behavior of the $B(E2; 0^+ \rightarrow 2^+)$ values in the silicon isotopes shows, from $N = 12$, a smooth decrease of collectivity as a function of neutron number with a minimum reached at $N = 20$. The collectivity then starts to increase as neutrons are added to the $N = 20$ closed shell. A microscopic angular momentum projection analysis of quadrupole collectivity in $^{32,34,36,38}\text{Si}$ with the Gogny interaction was undertaken by Rodriguez-Guzman *et al.* [13]. A comparison of their results with the experimental $B(E2)$ value [12] in ^{36}Si led them to conclude that a strong prolate component is present in the first 0^+ and 2^+ states.

So far, the only known excited state of ^{36}Si is the first 2^+ state with a large uncertainty in energy, 1399 ± 25 keV [12], studied by Coulomb excitation. For us to understand better the structure and nature of the collectivity of ^{36}Si , more

*Email address: xiaoying.liang@paisley.ac.uk

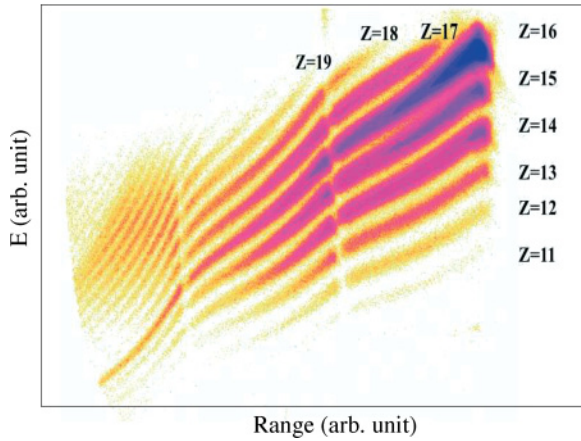


FIG. 1. (Color online) Energy vs range spectrum constructed from ionization chamber measurements, indicating the isotopes that were populated in the present work.

experimental data are needed on higher excited states, in particular the position of the first 4^+ state and the $E(4_1^+)$ to $E(2_1^+)$ ratio. Motivated by this need, we studied excited states in ^{36}Si by deep-inelastic processes in the present work. Our previous work [14] has shown that Doppler effects and lack of channel selection in thick target experiments limit the spectroscopy of projectile-like species. The combination of CLARA [15] and PRISMA [16–18] allows γ -ray detection in coincidence with projectile-like fragments in thin target experiments resulting in very clean channel selection and precise Doppler correction of γ -ray energies.

II. EXPERIMENT

Excited states of $N = 22$ ^{36}Si were populated in deep-inelastic processes produced by the interaction of a 215 MeV beam of ^{36}Si ions, delivered by the tandem-ALPI accelerator complex at the Legnaro National Laboratory, with a ^{208}Pb target. The target, isotopically enriched to 99.7% in ^{208}Pb , was of thickness $300 \mu\text{g cm}^{-2}$ on a $20 \mu\text{g cm}^{-2}$ C backing. Projectile-like nuclei produced here were detected

with PRISMA [16–18], a large solid angle (approximately 80 msr) magnetic spectrometer, placed at 56° to the beam direction, covering a range of angles including the grazing angle of the reaction. The PRISMA spectrometer consists of a quadrupole singlet and a dipole magnet separated by 60 cm. The (x, y) coordinates of an ion entering the spectrometer are measured using a position-sensitive MCP detector placed at 25 cm from the target. After passing the magnetic elements, the coordinates of the trajectory are measured again in the focal plane of the spectrometer using a ten-element 100 cm long multiwire PPAC. Finally, the ion is stopped in a 10×4 element ionization chamber used for Z and energy determination, from which the atomic charge state can be determined. Therefore, for each ion detected in PRISMA, we obtain the atomic number Z , the mass number A , and the ion charge state identification, thereby obtaining a very clean identification of all detected projectile-like isotopes.

γ rays from the deexcitation of the reaction products were detected using CLARA [15], an array of 25 escape-suppressed Ge Clover detectors (22 Ge Clover detectors were used during the experiment), in coincidence with projectile-like fragments detected by PRISMA. CLARA was positioned in the hemisphere opposite to the PRISMA spectrometer [16–18] and covering the azimuthal angles from 98° to 180° . Doppler correction of γ rays was performed on an event-by-event basis. The energy resolution of the γ -ray photopeaks following Doppler correction was typically around 0.6%. Experimental data were taken during a six day run.

III. RESULTS AND DISCUSSION

In the present work, we have populated a wide range of fragments, from Na ($Z = 11$) to Mn ($Z = 25$) as shown in Fig. 1. In this paper, we will focus on a discussion of Si isotopes. In the present work, we have populated $^{31-36}\text{Si}$. The mass spectrum obtained for the Si isotopes is shown in Fig. 2.

The γ -ray spectrum for ^{36}Si is shown in Fig. 3. Three γ rays with energies of 1408(1), 1442(3), and 842(1) keV are clearly observed here. The first $2^+ \rightarrow 0^+$ transition was previously observed in in-beam Coulomb excitation [12] with

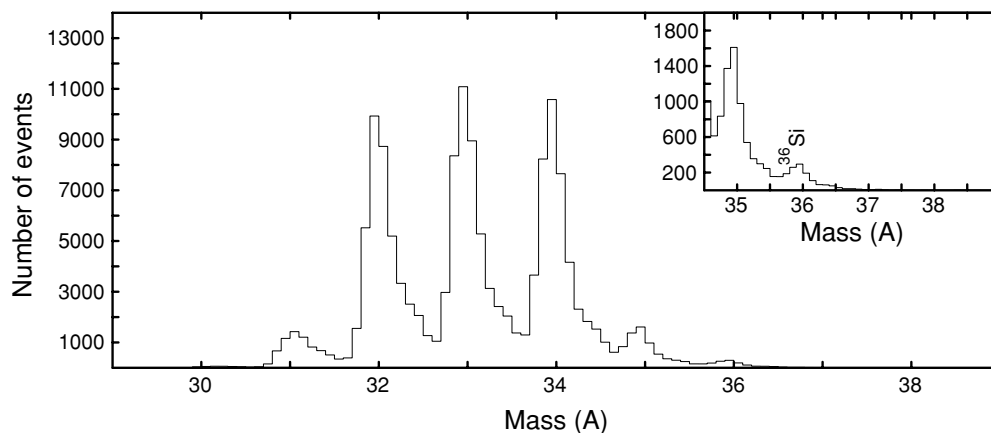
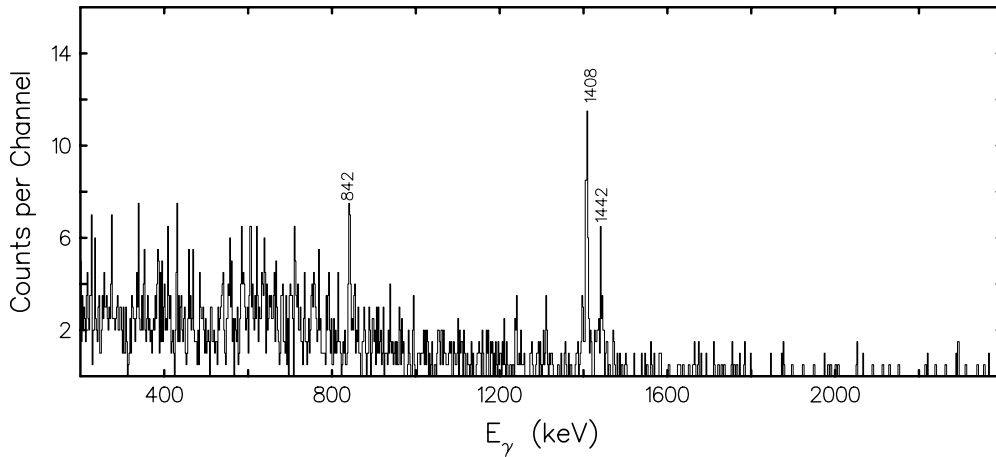


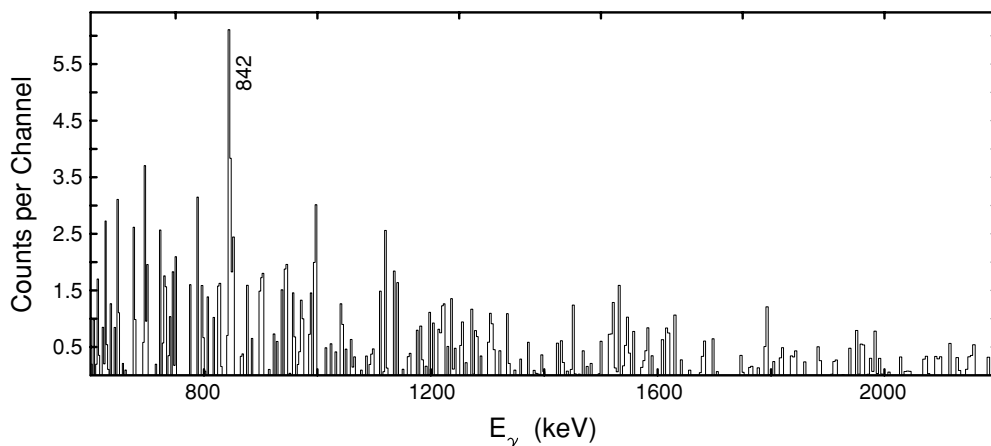
FIG. 2. Mass spectrum for Si isotopes populated in the present work.

FIG. 3. γ -ray spectrum for ^{36}Si .

an energy of 1399 ± 25 keV; the authors of this work produced neutron-rich Si isotopes by projectile fragmentation and γ rays were detected with NaI(Tl) detectors. This experimental technique and γ -ray detection array limited the accuracy of the measured γ -ray energy to ± 25 keV. In the present work, the energy of the $2^+ \rightarrow 0^+$ transition in ^{36}Si was measured with an accuracy of ± 1 keV. In addition to this, we observed two new transitions at energies of 1442 and 842 keV. In the present work, γ -ray coincidence measurements are not possible because of the low statistics in such a weak channel. Therefore, there is a potential uncertainty in relation to assigning the new transitions to a level scheme. However, we can resolve this problem by revisiting data from a previous thick target deep-inelastic experiment [10] which used the same projectile. In such an experiment, there is no ancillary detector for channel selection. In order to extract information on weakly populated channels, one has to rely on setting double gates on known γ -ray transitions. By double gating on transitions that are observed for the first time in the present work, we can obtain a better picture of the level scheme of ^{36}Si . Figure 4 shows one example of such a double-gated spectrum involving the 1408 and 1442 keV transitions; we can

clearly see a γ -ray photopeak at 842 keV. Therefore, we know that the three transitions at 1408, 1442, and 842 keV are in coincidence, and we tentatively assign the 1442 and 842 keV transitions as $4^+ \rightarrow 2^+$ and $6^+ \rightarrow 4^+$, respectively. The order of the transitions was determined by measuring of the relative γ -ray intensities.

To first-order approximation, the nucleus ^{36}Si , with 22 neutrons, has the two neutrons outside the $N = 20$ shell occupying the $1f_{7/2}$ orbital, leading to states with J^π values of 0^+ , 2^+ , 4^+ , and 6^+ . We have performed a large-scale shell model calculation for ^{36}Si using an *sdpf* model space, which fixed the protons in the *sd* shell and allowed the two extra-core neutrons to move in full *pf* orbitals. A comparison of our experimental level structure with the results of our shell model calculations is shown in Fig. 5. Here we used three different interactions: I(1) corresponds to the SDPF-NR interaction defined in the review paper by Caurier *et al.* [19], I(2) corresponds to a modified SDPF-NR interaction in which the *pf* shell pairing is reduced by 0.3 MeV, I(3) corresponds to a modified SDPF-NR interaction in which the *pf* shell pairing is reduced by 0.2 MeV and the $2p_{3/2}$ orbital energy is lowered by 1 MeV. We can see that a reduction of the *pf* shell

FIG. 4. γ -ray spectrum for ^{36}Si corresponding to a double gate on the 1408 and 1442 keV γ -ray photopeaks.

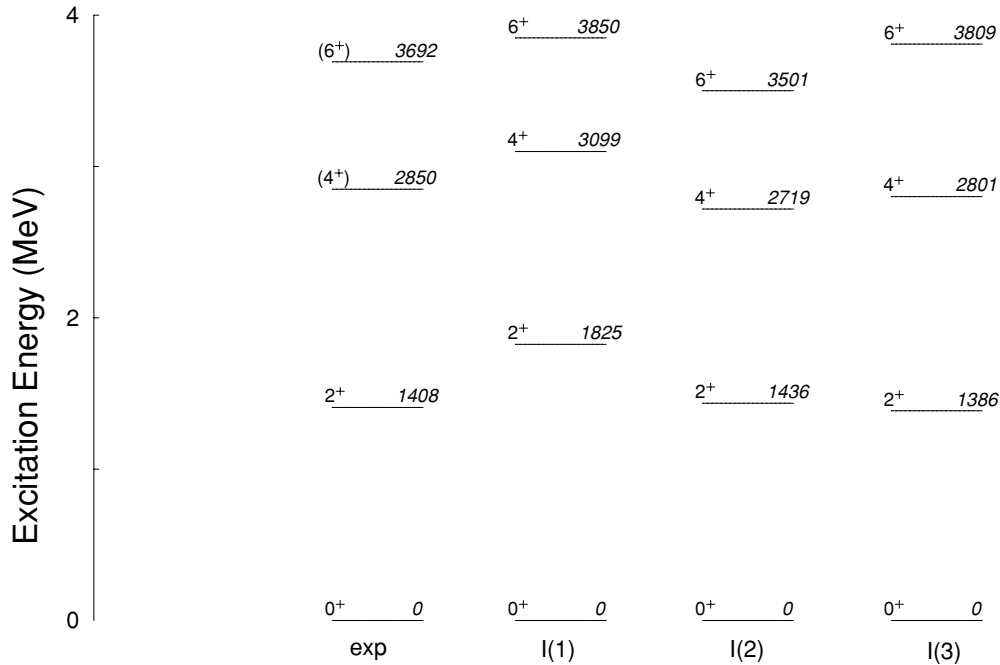


FIG. 5. Comparison of present experimental level scheme for ^{36}Si with the results of shell model calculations. See text for details.

pairing by 0.3 MeV is necessary to give us a correct 2^+ level energy. However, the 4^+ and 6^+ energies are too compressed using interaction I(2) when compared to the experimental data. Therefore, we modified the interaction further by reducing the $2p_{3/2}$ orbital single-particle energy by 1 MeV and reducing the pf shell pairing by 0.2 MeV [I(3)]. In interaction I(3), the reduction of the pf shell pairing by 0.2 MeV, rather than by 0.3 MeV as in interaction I(2), was necessary to reproduce the energy of the first 2^+ state. We can see that I(3) reproduces the experimental data well.

Figure 6 shows the systematics of the first 2^+ energies and experimental $B(E2; 0^+ \rightarrow 2^+)$ values in even- A Si, Mg, and S isotopes. Except for the first 2^+ energy of ^{36}Si , taken from the current work, and the experimental $B(E2; 0^+ \rightarrow 2^+)$ value for ^{34}Mg , taken from [20], all the 2^+ energies and experimental $B(E2; 0^+ \rightarrow 2^+)$ values were taken from [21]. There is a remarkable similarity in the first 2^+ energies in Si and S isotopes with $N \geq 16$; the addition of two protons outside the $1d_{5/2}$ orbital does not appear to have an influence on the energies of the first 2^+ states in the S isotopes. From Fig. 6 we can see that the $B(E2; 0^+ \rightarrow 2^+)$ value and $E(2^+)$ energy vary inversely to each other, as expected [22].

From Fig. 6, we clearly see that the systematic behavior of 2^+ energies and $B(E2; 0^+ \rightarrow 2^+)$ values for the Mg isotope is quite different from that for the Si and S isotopes. To understand this difference better, we also calculated the level energies and $B(E2)$ values for the $6^+ \rightarrow 4^+$, $4^+ \rightarrow 2^+$, and $2^+ \rightarrow 0^+$ transitions for the $N = 22$ ^{34}Mg , ^{36}Si , and ^{38}S isotones. The results are given in Table I where we list the results of shell model calculations using three different interactions I(1), I(2), and I(3). I(1) corresponds to the SDPF-NR interaction referred to above. I(2) corresponds to a modified SDPF-NR interaction in which the pf shell pairing

is reduced by 0.4, 0.3, and 0.2 MeV for ^{34}Mg , ^{36}Si , and ^{38}S , respectively. I(3) corresponds to a modified SDPF-NR interaction in which the $2p_{3/2}$ orbital energy is reduced by 1 MeV and the pf shell pairing is reduced by 0.3, 0.2, and 0.1 MeV for ^{34}Mg , ^{36}Si , and ^{38}S , respectively. We can see, as described earlier for the case of ^{36}Si , that a reduction of

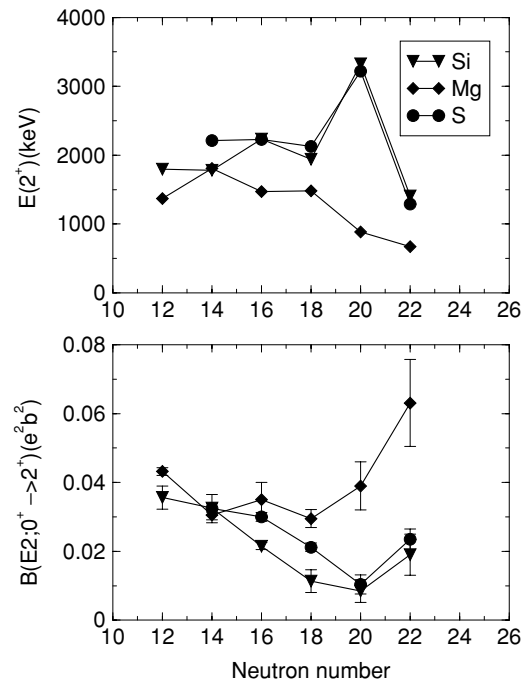


FIG. 6. Systematics of the first 2^+ energies and experimental $B(E2; 0^+ \rightarrow 2^+)$ values in even- A Si, Mg, and S isotopes with neutron numbers from 12 to 22.

TABLE I. Properties of the $N = 22$ neutron-rich Mg, Si, and S isotones. I(1) stands for the normal SDPF-NR interaction, I(2) and I(3) stand for modified SDPF-NR interactions as described in the text. Energies are in units of keV, $B(E2)$ values in units of $e^2 \text{fm}^4$.

| | ^{34}Mg | | | | ^{36}Si | | | | ^{38}S | | | |
|-----------------------|------------------|------|------|------|------------------|------|------|------|-----------------|------|------|------|
| | Exp. | I(1) | I(2) | I(3) | Exp. | I(1) | I(2) | I(3) | Exp. | I(1) | I(2) | I(3) |
| E_x | | | | | | | | | | | | |
| 2^+ | 658 | 1089 | 851 | 775 | 1408 | 1825 | 1436 | 1386 | 1292 | 1530 | 1298 | 1287 |
| 4^+ | 2118 | 2411 | 1984 | 1989 | 2850 | 3099 | 2719 | 2801 | 2826 | 2677 | 2376 | 2468 |
| 6^+ | | 3522 | 3073 | 3362 | 3692 | 3850 | 3501 | 3809 | 3675 | 3453 | 3149 | 3538 |
| $B(E2)$ | | | | | | | | | | | | |
| $2^+ \rightarrow 0^+$ | 108(20) | 89 | 91 | 94 | 39(12) | 45 | 51 | 48 | 47(6) | 51 | 51 | 54 |
| $4^+ \rightarrow 2^+$ | | 104 | 112 | 120 | | 41 | 48 | 49 | | 44 | 48 | 52 |
| $6^+ \rightarrow 4^+$ | | 89 | 97 | 108 | | 19 | 22 | 27 | | 44 | 46 | 55 |

the pf shell pairing [I(2)] is necessary to give us correct 2^+ level energies. To obtain better agreement for the 4^+ and 6^+ level energies with experimental results, we modified the interaction further, I(3). I(3), since we reduced the $2p_{3/2}$ orbital single-particle energy by 1 MeV, in order to keep the predicted 2^+ level energy to be the same as that predicted by I(2), the reduction of the pf shell pairing in I(3) is 0.1 MeV less than that in I(2). For $B(E2)$ values, there is no big difference between the three interactions. The way that the interaction was modified seems not to have changed the wave functions too much. For the three $N = 22$ isotones discussed here, the shell model values of $B(E2; 2^+ \rightarrow 0^+)$ are in very good agreement with experimental measurements [20,21]. In later discussion we will refer only to the predictions using I(3).

From Table I, we can see that there is a transition from deformation to spherical shape when we move from ^{34}Mg to ^{36}Si and ^{38}S . The shell model calculation predicts large $B(E2)$ values for all three transitions in ^{34}Mg , namely 94, 120, and 108 $e^2 \text{fm}^4$ for the $2^+ \rightarrow 0^+$, $4^+ \rightarrow 2^+$, and $6^+ \rightarrow 4^+$ transitions, respectively. So far, only the $2^+ \rightarrow 0^+$ $B(E2)$ experimental measurement in ^{34}Mg [20] is available, $108 \pm 20 e^2 \text{fm}^4$, and this is in very good agreement with

our prediction. The predicted large $B(E2)$ values in ^{34}Mg indicate that ^{34}Mg is a well-deformed nucleus. Indeed, this is confirmed from our shell model predictions for intrinsic frame quadrupole moments, $Q_0(s)$, which are extracted from the spectroscopic quadrupole moments, Q_{spec} . The detailed description for such a calculation can be found in Ref. [19]. The calculated $Q_0(s)$ values for ^{34}Mg are 64, 59, and 59 $e \text{fm}^2$ for the 2^+ , 4^+ , and 6^+ states, respectively. The nearly constant $Q_0(s)$ values indicate that ^{34}Mg is a good rotor. With two extra protons added to close the $1d_{5/2}$ proton orbital, ^{36}Si shows a nearly spherical shape behavior as is evidenced by a dramatic $B(E2)$ decrease compare with ^{34}Mg . By adding two more protons ^{38}S shows slightly more collectivity than ^{36}Si . Such a dramatic change from ^{34}Mg to ^{36}Si and ^{38}S is also confirmed by the data of Fig. 7 which shows the first 2^+ , 4^+ , and 6^+ level energies for the $N = 22$ isotones from Mg to Ca. We can see that there is a smooth change in level energies from Ca to Si, but the 2^+ and 4^+ energies decrease suddenly for ^{34}Mg . The $6^+ \rightarrow 4^+$ energy decreases as proton number increases; this

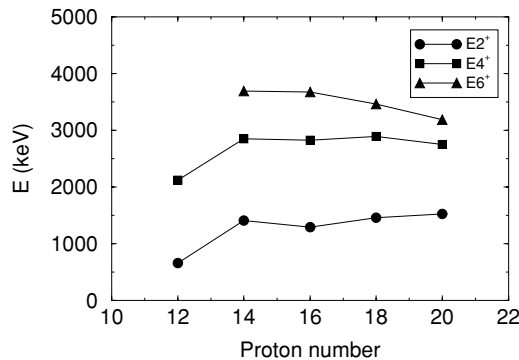


FIG. 7. Systematics of the first 2^+ , 4^+ , and 6^+ level energies for $N = 22$ isotones from Mg to Ca.

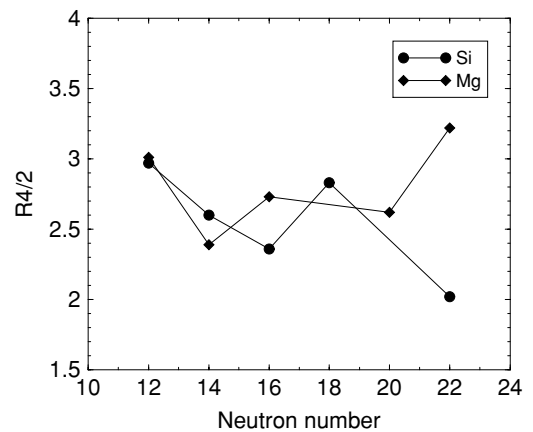


FIG. 8. Systematics of the $E(4_1^+)$ to $E(2_1^+)$ ratio, $R_{4/2}$, for Si and Mg isotopes with neutron numbers 12 to 22.

may be due to the proton particle-hole states as the $Z = 20$ shell closure is approached, as in the case of the ^{40}Ar and ^{42}Ca isotones.

The half-lives for states in ^{36}Si can also be deduced from the calculated $B(E2)$ values; they are 2.1, 1.8, and 49.8 ps for the 2^+ , 4^+ , and 6^+ states, respectively. These deduced half-lives are consistent with the observation of sharp γ -ray photopeaks corresponding to the decay of these three levels in our thick target deep-inelastic experiment. In a thick target deep-inelastic experiment, one can only observe γ -ray photopeaks corresponding to the decay of levels with lifetimes greater than about 1 ps. For those levels with lifetimes less than this value, the γ -ray photopeaks will be smeared out because of Doppler broadening. Experimental measurements of the lifetimes of the 2^+ , 4^+ , and 6^+ states in ^{36}Si would provide a very useful test of the present shell model calculations.

The present work allows us to obtain for the first time the $E(4_1^+)$ to $E(2_1^+)$ ratio in ^{36}Si , which is equal to 2.02. In ^{34}Mg the ratio is 3.22. The experimental $E(4_1^+)$ to $E(2_1^+)$ ratio together with the $B(E2)$ values predicted by the present shell model calculations lead us to conclude that ^{36}Si has a near-spherical shape. Figure 8 shows the systematics of the $E(4_1^+)$ to $E(2_1^+)$ ratio for Si and Mg isotopes with neutron numbers in the range of 12 to 22. We can see that at $N = 12$, the $E(4^+)$ to $E(2^+)$ ratios for Si and Mg are very similar, around 3.0. However, the $E(4^+)$ to $E(2^+)$ ratios for Si and Mg start to differ as neutrons

are added, and the largest difference is reached at $N = 22$. (We should note here that no experimental $E(4^+)$ to $E(2^+)$ ratio is available for $N = 20$ ^{32}Mg .)

IV. CONCLUSIONS

The yrast decay sequence for ^{36}Si has been observed for the first time up to the 6^+ state. The level energies were compared with the results of *sdpf* shell model calculations using a modified SDPF-NR interaction, and the observed states are well reproduced. From the experimental $E(4_1^+)$ to $E(2_1^+)$ ratio together with the $B(E2)$ values predicted by shell model calculations obtained in the present work, we conclude that ^{36}Si has a near-spherical shape. The behavior of ^{36}Si is very different from the neighboring even- Z ^{34}Mg . Observation of the three γ -ray transitions reported here in a previous thick target experiment indicates that the lifetimes of these three levels are greater than about 1 ps; this is also consistent with the results of our shell model calculations.

ACKNOWLEDGMENTS

This work was supported in part by an EPSRC (U.K.) grant. Three of us, A.H., K.K., and A.P., also acknowledge support from the EPSRC.

-
- [1] T. Motobayashi, Y. Ikeda, Y. Ando, K. Ieki, M. Inoue, N. Iwasa, T. Kikuchi, M. Kurokawa, S. Moriya, S. Ogawa, H. Murakami, S. Shimoura, Y. Yanagisawa, T. Nakamura, Y. Watanabe, M. Ishihara, T. Teranishi, H. Okuno, and R. F. Casten, *Phys. Lett.* **B346**, 9 (1995).
- [2] B. V. Pritychenko, T. Glasmacher, P. D. Cottle, M. Fauerbach, R. W. Ibbotson, K. W. Kemper, V. Maddalena, A. Navin, R. Ronningen, A. Sakharuk, H. Scheit, and V. G. Zelevinsky, *Phys. Lett.* **B461**, 322 (1999).
- [3] V. Chiste, A. Gillibert, A. Lepine-Szily, N. Alamanos, F. Auger, J. Barrette, F. Braga, M. D. Cortina-Gil, Z. Dlouhy, V. Lapoux, M. Lewitowicz, R. Lichtenthaler, R. Liguori Neto, S. M. Lukyanov, M. MacCormick, F. Marie, W. Mittig, F. de Oliveira Santos, N. A. Orr, A. N. Ostrowski, S. Ottini, A. Pakou, Yu. E. Penionzhkevich, P. Roussel-Chomaz, and J. L. Sida, *Phys. Lett.* **B514**, 233 (2001).
- [4] E. K. Warburton, J. A. Becker, and B. A. Brown, *Phys. Rev. C* **41**, 1147 (1990).
- [5] A. Poves and J. Retamosa, *Phys. Lett.* **B184**, 311 (1987); A. Poves and J. Retamosa, *Nucl. Phys.* **A571**, 221 (1994).
- [6] T. Glasmacher, B. A. Brown, M. J. Chromik, P. D. Cottle, M. Fauerbach, R. W. Ibbotson, K. W. Kemper, D. J. Morrissey, H. Scheit, D. W. Sklenicka, and M. Steiner, *Phys. Lett.* **B395**, 163 (1997).
- [7] H. Scheit, T. Glasmacher, B. A. Brown, J. A. Brown, P. D. Cottle, P. G. Hansen, R. Harkewicz, M. Hellstrom, R. W. Ibbotson, J. K. Jewell, K. W. Kemper, D. J. Morrissey, M. Steiner, P. Thierolf, and M. Thoennessen, *Phys. Rev. Lett.* **77**, 3967 (1996).
- [8] T. R. Werner, J. A. Sheikh, M. Misu, W. Nazarewicz, J. Rikowska, K. Heeger, A. S. Umar, and M. R. Strayer, *Nucl. Phys.* **A597**, 327 (1996).
- [9] X. Liang, R. Chapman, F. Haas, K.-M. Spohr, P. Bednarczyk, S. M. Campbell, P. J. Dagnall, M. Davison, G. de Angelis, G. Duchene, Th. Kroll, S. Lunardi, S. Naguleswaran, and M. B. Smith, *Phys. Rev. C* **66**, 037301 (2002).
- [10] J. Ollier, R. Chapman, X. Liang, M. Labiche, K.-M. Spohr, M. Davison, G. de Angelis, M. Axiotis, T. Kroll, D. R. Napoli, T. Martinez, D. Bazzacco, E. Farnea, S. Lunardi, and A. G. Smith, *Phys. Rev. C* **67**, 024302 (2003).
- [11] J. Retamosa, E. Caurier, F. Nowacki, and A. Poves, *Phys. Rev. C* **55**, 1266 (1997).
- [12] R. W. Ibbotson, T. Glasmacher, B. A. Brown, L. Chen, M. J. Chromik, P. D. Cottle, M. Fauerbach, K. W. Kemper, D. J. Morrissey, H. Scheit, and M. Thoennessen, *Phys. Rev. Lett.* **80**, 2081 (1998).
- [13] R. Rodriguez-Guzman, J. L. Egido, and L. M. Robledo, *Phys. Lett.* **B474**, 15 (2000).
- [14] X. Liang, Ph.D. thesis, University of Paisley, 2002 (unpublished).
- [15] A. Gadea, D. R. Napoli, G. Angelis, R. Menegazzo, A. M. Stefanini, L. Corradi, M. Axiotis, L. Berti, E. Fioretto, T. Kroell, A. Latina, N. Marginean, G. Maron, T. Martinez, D. Rosso, C. Rusu, N. Toniolo, S. Szilner, M. Trotta, D. Bazzacco, S. Beghini, M. Bellato, F. Brandolini, E. Farnea, R. Isocrate, S. M. Lenzi, S. Lunardi, G. Montagnoli, P. Pavan, C. Rossi Alvarez, F. Scarlassara, C. Ur, N. Blasi, A. Bracco, F. Camera, S. Leoni, B. Million, M. Pignanelli, G. Pollarolo,

- A. DeRosa, G. Inghima, M. Commaro, G. Rana, D. Pierroussakou, M. Romoli, M. Sandoli, P. G. Bizzeti, A. M. Bizzeti-Sona, G. Lo Bianco, C. M. Petrache, A. Zucchiatti, P. Cocconi, B. Quintana, Ch Beck, D. Curien, G. Duchene, F. Haas, P. Medina, P. Papka, J. Durell, S. J. Freeman, A. Smith, B. Varley, K. Fayz, V. Pucknell, J. Simpson, W. Gelletly, and P. Regan, *Eur. Phys. J. A* **20**, 193 (2004).
- [16] A. M. Stefanini, L. Corradi, G. Maron, A. Pisent, M. Trotta, A. M. Vinodkumar, S. Beghini, G. Montagnoli, F. Scarlassara, G. F. Segato, A. De Rosa, G. Inghima, D. Pierroussakou, M. Romoli, M. Sandoli, G. Pollarolo, and A. Latina, *Nucl. Phys. A* **701**, 217c (2002).
- [17] G. Montagnoli, A. M. Stefanini, M. Trotta, S. Beghini, M. Bettini, F. Scarlassara, V. Schiavon, L. Corradi, B. R. Behera, E. Fioretto, A. Gadea, A. Latina, S. Szilner, D. L. Don, M. Rigato, N. A. Kondratiev, A. Yu. Chizhov, G. Kniajeva, E. M. Kozulin, I. V. Pokrovskiy, V. M. Voskressensky, and D. Ackermann, *Nucl. Instrum. Methods Phys. Res. A* **547**, 455 (2005).
- [18] S. Beghini, L. Corradi, E. Fioretto, A. Gadea, A. Latina, G. Montagnoli, F. Scarlassara, A. M. Stefanini, S. Szilner, M. Trotta, and A. M. Vinodkumar, *Nucl. Instrum. Methods Phys. Res. A* **551**, 364 (2005).
- [19] E. Caurier, G. Martinez-Pinedo, F. Nowacki, A. Poves, and A. P. Zuker, *Rev. Mod. Phys.* **77**, 427 (2005).
- [20] H. Iwasaki, T. Motobayashi, H. Sakurai, K. Yoneda, T. Gomi, N. Aoi, N. Fukuda, Zs. Fulop, U. Futakami, Z. Gacsi, Y. Higurashi, N. Imai, N. Iwasa, T. Kubo, M. Kunibu, M. Kurokawa, Z. Liu, T. Minemura, A. Saito, M. Serata, S. Shimoura, S. Takeuchi, Y. X. Watanabe, K. Yamada, Y. Yanagisawa, and M. Ishihara, *Phys. Lett.* **B522**, 227 (2001).
- [21] S. Raman, C. W. Nestor, and P. Tikkanen, Jr., *At. Data Nucl. Data Tables* **78**, 1 (2001).
- [22] L. Grozins, *Phys. Lett.* **2**, 88 (1962).